

Stable State Space SubSpace (S^5) Identification

Xinhui Rong and Victor Solo *

August 19, 2024

Abstract

State space subspace algorithms for input-output systems have been widely applied but also have a reasonably well-developed asymptotic theory dealing with consistency. However, guaranteeing the stability of the estimated system matrix is a major issue. Existing stability-guaranteed algorithms are computationally expensive, require several tuning parameters, and scale badly to high state dimensions. Here, we develop a new algorithm that is closed-form and requires no tuning parameters. It is thus computationally cheap and scales easily to high state dimensions. We also prove its consistency under reasonable conditions.

Copyright Statement

This work has been submitted to the IEEE for possible publication. Copyright may be transferred without notice, after which this version may no longer be accessible.

1 Introduction

There are two types of linear state space (SS) model relevant to system identification. In input-output SS (IO-SS) models, the states are driven by unmeasured noise and measured input signals. In state space noise (N-SS) models, the state is driven only by an unmeasured noise.

* Authors are with School of Electrical Eng. & Telecommunications, UNSW, Sydney, Australia.

The state space subspace (S^4) approach is a powerful method of SS modelling, applicable to both IO-SS and N-SS models. It does not rely on parameterization and avoids identifiability issues. The S^4 method uses projection theorems to extract the state or a system-related matrix, namely the state sequence or the extended observability matrix, from the input and output signals (or only the output signal in the N-SS case) [32], followed by various methods to identify the system matrices. The S^4 method is of great interest due to its simple implementation and calculation; it involves little more than singular value decomposition (SVD).

S^4 identification with guaranteed system stability has long been of interest since unstable identification can occur on systems that are known to be stable, due to limited measurement time, or noise. The simpler system structure of the N-SS models allows a wider range of stability-guaranteed algorithms as the state equation is a first-order vector autoregression (VAR(1)).

For N-SS models, Mari et al. [16] consider a semidefinite programming (SDP) problem with Lyapunov stability constraint to minimize the weighted discrepancy between the unstable initial estimate and the stable one. We shall refer to such method the *perturbation minimization*. Boots et al. [2] use a constraint generation approach which minimizes the norm of the one-step-ahead prediction error under a singular value constraint that is iteratively restricted until a stable solution is reached. Tanaka and Katayama [29] also use the perturbation minimization procedure and stabilize the state transition matrix by solving Riccati equations. Jongeneel et al. [10] propose a new LQR problem and offer error analysis and statistical guarantees for the VAR(1) problem. However, in the N-SS setting, the necessity to invert the mean square error sample matrix in the algorithm can lead to operational challenges when it approaches singularity as is often the case in the simulations. We [23] use a *forwards-backwards (FB) optimization* [3] [28] [20] on the error residuals whose solution is closed-form and guaranteed stable for N-SS. We further extended the work to encompass symmetry [26] and rank constraints [25]. More recently, we [24] developed for VAR(1) a class of *correlation stable estimators*, which are stable, closed-form and consistent.

For IO-SS models, Chui and Maciejowski [4] use an iterative attenuation (IA) method where the estimated state sequence or the extended observability matrix is iteratively appended until stability is reached. However, this method distorts the estimator and introduces additional bias, since the estimator will have a dominating pole with a user-defined magnitude. Van Gestel et al. [31] develop

the regularization method to the standard least squares to guarantee stability. Lacy and Bernstein [12] extend the SDP method to include input. Mallet et al. [15] use a line search method based on gradient sampling. Umenberger et al. [30] use the expectation maximization (EM) method. However, it is too computationally expensive since there is a SDP procedure in every iteration of EM.

More recently another approach to guaranteed stability has appeared. The idea is to find the nearest stable matrix to the initial unstable estimate [21] [7] [19]. However, they can only guarantee a local minimum and no data information is used except for the initial unstable estimate.

Stability-guaranteed algorithms for IO-SS can be adapted to N-SS (see [23] for examples), but the reverse is not straightforward. For example, the SDP methods in [16] and [12] end up being the same even though an input is considered in [12]. However, the LQR method in [10] requires that the state and noise covariance matrices obey a Lyapunov equation associated with the state transition matrix which only occurs in the noise modeling or VAR(1).

In this paper, we consider IO-SS modelling with a VAR(1) input process and extend the correlation stable estimators [24] to encompass such system structure. We develop the first closed-form, tuning-parameter-free stable S^4 , which we call S^5 , that can be applied to both IO-SS and N-SS. We also show statistical consistency for S^5 under reasonable conditions.

The rest of the paper is organized as follows. We first introduce the IO-SS model in Section 2. We review canonical variate analysis (CVA) subspace identification of the states in Section 3, and the correlation stable estimators for VAR(1) in Section 4. We then develop

- (i) in Section 5, the S^5 algorithm,
- (ii) in Section 6, statistical consistency for the S^5 estimator.

We compare S^5 with various previous methods in simulations in Section 7 with both low-dimensional and high-dimensional examples.

We define the following notations. A' is the transpose of A . $\rho(A)$ is the spectral radius of A , i.e. the largest modulus of the eigenvalues. $\|A\| = \sqrt{\text{tr}(AA')}$ is the Frobenius norm of A . \otimes is the Kronecker product. I_k is the identity matrix with dimension k , or I the identity matrix with appropriate dimension. \xrightarrow{P} means convergence in probability. w.p.1 means ‘with probability 1’.

2 State Space Modeling

We consider the linear, time-invariant SS model in the innovations form

$$x_{t+1} = Ax_t + Bu_t + K\epsilon_t \quad (2.1a)$$

$$y_t = Cx_t + \epsilon_t, \quad (2.1b)$$

where y_t is the d -vector measured output, u_t is the m -vector measured input, x_t is the n -vector latent state. The innovation ϵ_t is white, i.e. $E[\epsilon_t \epsilon_s'] = 0, t \neq s$, with zero mean and covariance $E[\epsilon_t \epsilon_t'] = Q_\epsilon > 0$. The matrices $A_{n \times n}, B_{n \times m}, C_{d \times n}, K_{n \times d}$ contain the system parameters, where $K_{n \times d}$ is the Kalman gain. We introduce some assumptions for the SS model.

Assumption A1. For the SS model (2.1),

- The ϵ_t and u_t sequences are statistically independent.
- A and $A - KC$ are stable $\equiv \rho(A) < 1, \rho(A - KC) < 1$.
- (A, C) is observable, $(A, [K, B])$ is reachable.

Note that $\rho(A - KC) < 1$ means the system is minimum-phase, and A1 ensures the state space representation (2.1) is minimal [8, Theorem 2.3.4].

Further assumptions on e_t are needed for the asymptotic analysis below.

Assumption A2. For the innovation sequence ϵ_t .

- $E[\epsilon_t | \mathcal{F}_{t-1}^\epsilon] = 0, E[\epsilon_t \epsilon_t' | \mathcal{F}_{t-1}^\epsilon] = E[\epsilon_t \epsilon_t'] > 0$ under the history $\mathcal{F}_t^\epsilon = \sigma\{\epsilon_t, \epsilon_{t-1}, \dots\}$.
- $E[\epsilon_{t,a}^4] < \infty, E[\epsilon_{t,a} \epsilon_{t,b} \epsilon_{t,c} | \mathcal{F}_{t-1}^\epsilon] = \omega_{a,b,c}$, where $\epsilon_{t,a}$ is the a -th entry in ϵ_t and $\omega_{a,b,c}$ is a constant independent from t .

We now introduce assumptions on the input sequence.

Assumption A3. Input is VAR(1).

u_t obeys the VAR(1) model,

$$u_{t+1} = A_u u_t + v_t, \quad (2.2)$$

where A_u is the $m \times m$ stable VAR(1) matrix, and v_t is an iid zero mean white noise sequence with covariance $Q_v = E[v_t v_t'] > 0$. We further assume: (i) v_t satisfies A2 (with history \mathcal{F}_t^v); and (ii) A and A_u have no common eigenvalues.

Remarks 1.

- (i) Note that in view of A1, the sequences ϵ_t, v_t are statistically independent.

- (ii) It is straightforward to show that any sequence of the form $w_t = D_1\epsilon_t + D_2v_t$ (for constant matrices D_1, D_2) also obeys A2 (with history \mathcal{F}_t^w).

Taking variances in (2.2) and assuming stationarity we find that the variance matrix $\Pi_u \equiv \mathbb{E}[u_t u_t']$ obeys the Lyapunov equation: $\Pi_u = A_u \Pi_u A_u' + Q_v > 0$. Further, introducing the lag 1 covariance $\Pi_{u,10} = \mathbb{E}[u_{t+1} u_t']$, we find $A_u = \Pi_{u,10} \Pi_u^{-1}$.

We aim to estimate the system matrices (A, B, C, K) , the innovation covariance Q_ϵ and the VAR matrices A_u, Q_v and require the estimated A and A_u to be stable.

3 Review of Canonical Variate Analysis State Space Subspace Method

The S^4 methods use projections to estimate the unobserved states [32], which are later used for system identification. In this section, we briefly review the canonical variate analysis (CVA) subspace method [13].

First, introduce the lag- p stacked past input vector $u_{t,p}^- = [u_{t-1}' \dots u_{t-p}']'$ and the lag- f future input vector $u_{t,f}^+ = [u_t' \dots u_{t+f-1}']'$. Also define similarly the past and future output vector, $y_{t,p}^-$ and $y_{t,f}^+$ and $z_{t,p}^- = [(y_{t,p}^-)', (u_{t,p}^-)']'$ and $\bar{A} = A - KC$. Using the SS innovation form (2.1), one can easily obtain

$$x_t = \bar{A}^p x_{t-p} + \mathcal{K}_p z_{t,p}^-, \quad (3.1)$$

where $\mathcal{K}_p = [K, B, \bar{A}[K, B], \bar{A}^2[K, B], \dots, \bar{A}^{p-1}[K, B]]$ is the extended controllability matrix and has full row rank by the minimality A1 given $p \geq n$. Also,

$$y_{t,f}^+ = \mathcal{O}_f x_t + \Phi_f u_{t,f}^+ + \eta_{t,f}^+ \quad (3.2a)$$

$$= \mathcal{O}_f \mathcal{K}_p z_{t,p}^- + \mathcal{O}_f \bar{A}^p x_{t-p} + \Phi_f u_{t,f}^+ + \eta_{t,f}^+, \quad (3.2b)$$

where $\mathcal{O}_f = [C', A'C', \dots, (A^{f-1})'C']'$ is the extended observability matrix, Φ_f is lower block triangular and contains the system matrices, and $\eta_{t,f}^+$ is related to the future noise and is independent from the remaining terms. Also note that $\mathcal{O}_f \mathcal{K}_p$ will be of low rank n for sufficiently large f, p .

The minimum-phase assumption in A1 enables the approximation of x_t as

a linear transformation of $z_{t,p}^-$ as

$$x_t \approx \mathcal{K}_p z_{t,p}^-, \quad (3.3)$$

so that one can write $y_{t,f}^+ = \beta_z z_{t,p}^- + \beta_u u_{t,f}^+ + r_{t,f}^+$ where β_u is some constant matrix, $r_{t,f}^+$ is the residual term which is in general not orthogonal to $z_{t,p}^-$ and $u_{t,f}^+$, and

$$\beta_z = \mathcal{O}_f(\mathcal{K}_p + \bar{A}^p D), \quad (3.4)$$

where D is a finite term. However, the minimum-phase assumption ensures the bias between β_z and $\mathcal{O}_f \mathcal{K}_p$ vanishes as $p \rightarrow \infty$ (at a certain rate, see Section 6).

Motivated by (3.3), CVA predicts x_t as linear combination of $z_{t,p}^-$ as $\hat{x}_t = \hat{\mathcal{K}}_p z_{t,p}^-$, and minimizes the noise in (3.2a), regressed on $u_{t,f}^+$ as follows.

Given the input-output data for $t = 0, \dots, \bar{T}$, choose the lags $p \geq n, f \geq n$ and define $T = \bar{T} - f - p + 1$, and the past and future data matrices $Z_p^- = [z_{p,p}^-, \dots, z_{p+T,p}^-]$, $Y_f^+ = [y_{p,p}^+, \dots, y_{p+T,f}^+]$, $U_f^+ = [u_{p,p}^+, \dots, u_{p+T,f}^+]$. Under A3, $U_f^+ (U_f^+)'$ has full rank w.p.1. We also define the projection matrices

$$\begin{aligned} \Pi_U &= U'(UU')^{-1}U \\ \text{and } \Pi_U^\perp &= I - \Pi_U. \end{aligned}$$

$Y\Pi_U$ projects the row space of Y onto the row space of U and $Y\Pi_U^\perp$ is the residual. Π_U^\perp has properties such that $(\Pi_U^\perp)^2 = \Pi_U^\perp$ and $U\Pi_U^\perp = 0$.

Let $\hat{X} = [\hat{x}_p, \dots, \hat{x}_{p+T}]$, which is to be found. Then, by partial regression and (3.2a), we estimate \mathcal{O}_f as

$$\hat{\mathcal{O}}_f = Y_f^+ \Pi_{U_f^+}^\perp \hat{X}' (\hat{X} \Pi_{U_f^+}^\perp \hat{X}')^{-1},$$

and predict $y_{t,f}^+$ as

$$\hat{Y}_f^+ = \hat{\mathcal{O}}_f \hat{X} + \hat{\Phi}_f U_f^+ \Rightarrow \hat{Y}_f^+ \Pi_{U_f^+}^\perp = \hat{\mathcal{O}}_f \hat{X} \Pi_{U_f^+}^\perp,$$

where $\hat{\Phi}_f$ is some estimate of Φ_f but is not needed here since it vanishes in the projection. Then the optimization problem becomes finding $\hat{\mathcal{K}}_p$ such that $\hat{X} = \hat{\mathcal{K}}_p Z_p^-$, and $\|W^{-\frac{1}{2}}(Y_f^+ - \hat{Y}_f^+) \Pi_{U_f^+}^\perp\|^2$ is minimized, where W is a positive definite weighting matrix. The solution is given below. Let $W = \hat{\Sigma}_{ff}^\perp =$

$\frac{1}{T}Y_f^+\Pi_{U_f^+}^\perp(Y_f^+)'$, $\hat{\Sigma}_{fp}^\perp = \frac{1}{T}Y_f^+\Pi_{U_f^+}^\perp(Z_p^-)'$ and $\hat{\Sigma}_{pp}^\perp = \frac{1}{T}Z_p^-\Pi_{U_f^+}^\perp(Z_p^-)'$. Carry out the SVD

$$(\hat{\Sigma}_{ff}^\perp)^{-\frac{1}{2}}\hat{\Sigma}_{fp}^\perp(\hat{\Sigma}_{pp}^\perp)^{-\frac{1}{2}} = \hat{U}\hat{\Lambda}\hat{V}' = [\hat{U}_{\hat{n}}, \hat{U}_*] \begin{bmatrix} \hat{\Lambda}_{\hat{n}} & 0 \\ 0 & \hat{\Lambda}_* \end{bmatrix} \begin{bmatrix} \hat{V}'_{\hat{n}} \\ \hat{V}'_* \end{bmatrix},$$

where $G^{\frac{1}{2}}$ is the unique symmetric matrix square root of a positive definite (pd) G and $\hat{\Lambda}_{\hat{n}}$ contains the largest \hat{n} singular values in decreasing order down its diagonal, where $\hat{n} \leq f$ is the estimated state dimension and \hat{U}, \hat{V} are normalized singular vectors. Then,

$$\hat{\mathcal{K}}_p = \hat{\Lambda}_{\hat{n}}^{\frac{1}{2}}\hat{V}'_{\hat{n}}(\hat{\Sigma}_{pp}^\perp)^{-\frac{1}{2}} \quad (3.5)$$

$$\Rightarrow \hat{X} = \hat{\mathcal{K}}_p Z_p^-. \quad (3.6)$$

We note here for future use that $\hat{\mathcal{O}}_f = (\hat{\Sigma}_{ff}^\perp)^{\frac{1}{2}}\hat{U}_{\hat{n}}\hat{\Lambda}_{\hat{n}}^{\frac{1}{2}}$ and $\hat{\mathcal{O}}_f\hat{\mathcal{K}}_p$ is the rank n approximation of

$$\hat{\beta}_z = \hat{\Sigma}_{fp}^\perp(\hat{\Sigma}_{pp}^\perp)^{-1}, \quad (3.7)$$

the estimator for β_z by partial regression without rank constraint. Thus, an alternative expression for $\hat{\mathcal{K}}_p$ is [32] $\hat{\mathcal{K}}_p = \hat{\mathcal{O}}_f^\dagger\hat{\beta}_z$, where

$$\hat{\mathcal{O}}_f^\dagger = (\hat{\mathcal{O}}_f'(\hat{\Sigma}_{ff}^\perp)^{-1}\hat{\mathcal{O}}_f)^{-1}\hat{\mathcal{O}}_f'(\hat{\Sigma}_{ff}^\perp)^{-1} = \hat{\Lambda}_{\hat{n}}^{-\frac{1}{2}}\hat{U}'_{\hat{n}}(\hat{\Sigma}_{ff}^\perp)^{-\frac{1}{2}},$$

is the left pseudo inverse of $\hat{\mathcal{O}}_f$. This will simplify the discussion of asymptotics a lot.

After getting the estimated states, system matrices A, B, C, K can be estimated by least squares (LS). Let $\hat{X}_1 = [\hat{x}_{p+1}, \dots, \hat{x}_{p+T}]$, $\hat{X}_0 = [\hat{x}_p, \dots, \hat{x}_{p+T-1}]$, $Y_0 = [y_p, \dots, y_{p+T-1}]$, and $U_0 = [u_p, \dots, u_{p+T-1}]$. Then, the LS estimators of A, B, C are

$$\begin{bmatrix} \hat{A}_* & \hat{B} \end{bmatrix} = \hat{X}_1 \begin{bmatrix} \hat{X}'_0 & U'_0 \end{bmatrix} \left(\begin{bmatrix} \hat{X}'_0 \\ U'_0 \end{bmatrix} \begin{bmatrix} \hat{X}'_0 & U'_0 \end{bmatrix} \right)^{-1} \quad (3.8)$$

$$\hat{C} = Y_0 X'_0 (X_0 X'_0)^{-1}. \quad (3.9)$$

Note that \hat{A}_* is not guaranteed to be stable w.p.1. For future use we note that

$$\hat{A}_* = \hat{X}_1 \Pi_{\hat{U}_0}^\perp \hat{X}'_0 (\hat{X}_0 \Pi_{\hat{U}_0}^\perp \hat{X}'_0)^{-1}. \quad (3.10)$$

Let $\hat{E} = Y_0 - \hat{C}\hat{X}_0$. The LS estimator of K is $\hat{K} = \hat{X}_1 \hat{E}' (\hat{E} \hat{E}')^{-1}$. The estimator of Q_ϵ is $\frac{1}{T} \hat{E} \hat{E}'$.

4 Correlation Stable VAR(1) Estimators

Our new closed-form stable estimator (S^5) builds on closed-form stable estimators for VAR(1) models. These are developed in our recent work [24] and are called *correlation stable* (CS) estimators.

Let the n -vector process ξ_t be a VAR(1) process

$$\xi_{t+1} = F\xi_t + w_t, \quad (4.1)$$

with F stable and w_t a zero mean white noise sequence with covariance $Q_w > 0$.

Then as indicated below A3, under stationarity, the state covariance satisfies a Lyapunov equation $E[\xi_t \xi_t'] = \Pi_\xi = F \Pi_\xi F' + Q_w > 0$.

Introduce $Z = [\xi_p, \xi_{p+1}, \dots, \xi_{p+T}]$ and Z_0 to be Z without the last column and Z_1 to be Z without the first column. Also introduce the sample covariance matrices

$$S_{\xi,ij} = \frac{1}{T} Z_i Z_j', \quad i, j \in \{0, 1\}. \quad (4.2)$$

The CS estimator is given in the following theorem.

Theorem 1. [24] Correlation Stable (CS) Estimator for VAR(1). Suppose that ξ_t satisfies the stable VAR(1) given in (4.1) and that w_t 's are iid with mean 0, covariance $\Pi_\xi > 0$ and finite fourth moment. Let P be any positive definite consistent estimator of Π_ξ . The following estimator of F is stable and consistent.

$$\hat{F}_P = P^{\frac{1}{2}} R P^{-\frac{1}{2}} \xrightarrow{p} F, \quad (4.3)$$

where $R = S_{\xi,11}^{-\frac{1}{2}} S_{\xi,10} S_{\xi,00}^{-\frac{1}{2}}$ is the correlation matrix.

Proof. [24, Theorem IVb] For completeness and later extension, we repeat part of the proof here. Firstly note that the eigenvalues of \hat{F}_P are the same as those of R since $|\lambda I - \hat{F}_P| = |\lambda I - R|$. Next $\rho(R) \leq \sigma(R) \equiv$ largest singular

value of R [9, Chapter 4]. But by the Cauchy-Schwartz inequality [17, Theorem 11.2] $\sigma(R) < 1$ w.p.1. The stability now follows. \square

Corollary 1. Setting $P = S_{\xi,11}$ we get

$$\hat{F} = S_{\xi,10} S_{\xi,00}^{-\frac{1}{2}} S_{\xi,11}^{-\frac{1}{2}} \xrightarrow{P} F. \quad (4.4)$$

5 Stable State Space Subspace Identification

We now consider extending the CS estimator to IO-SS models.

5.1 Markovian State Extraction

First note that the VAR(1) in A3 can be written as a SS model as follows

$$\zeta_{t+1} = A_u \zeta_t + A_u v_{t-1} \text{ and } u_t = \zeta_t + v_{t-1}$$

where ζ_t is an unobserved state.

We can now form a joint SS model as follows.

$$\begin{bmatrix} x_{t+1} \\ \zeta_{t+1} \end{bmatrix} = \begin{bmatrix} A & B \\ 0 & A_u \end{bmatrix} \begin{bmatrix} x_t \\ \zeta_t \end{bmatrix} + \begin{bmatrix} K \epsilon_t \\ A_u v_{t-1} \end{bmatrix} \quad (5.1a)$$

$$\begin{bmatrix} y_t \\ u_t \end{bmatrix} = \begin{bmatrix} C & 0 \\ 0 & I \end{bmatrix} \begin{bmatrix} x_t \\ \zeta_t \end{bmatrix} + \begin{bmatrix} \epsilon_t \\ v_{t-1} \end{bmatrix}. \quad (5.1b)$$

Since we now have a noise driven SS model, we could try to apply the stability guaranteed method we developed in [24]. But that method cannot handle the constraint that the left bottom corner block entry in the system matrix is 0. We have instead been led to find a different approach.

It turns out to be possible to construct a new state whose transition matrix is A .

Result I. Assume x_t, u_t satisfy (2.1) and (2.2) and the assumptions A1-A3 are fulfilled. Introduce $M_{n \times m}$ which solves the Sylvester equation

$$AM - MA_u + B = 0. \quad (5.2)$$

Then $\xi_t = x_t - M u_t$ satisfies a VAR(1) taking the form

$$\xi_{t+1} = A \xi_t + w_t, \quad w_t = K \epsilon_t - M v_t. \quad (5.3)$$

Remarks 2.

- (i) From now on we will be using the notation and results of Section IV so are effectively setting $F = A$.
- (ii) The Sylvester equation (5.2) has a unique solution M iff A and A_u do not have common eigenvalues [5, Ch.8]. This is guaranteed by A3.
- (iii) w_t is white and not correlated to ξ_t , so ξ_t is bona-fide Markovian state sequence. Note that w_t has covariance $Q_w = KQ_\epsilon K' + MQ_v M' \geq 0$.
- (iv) In steady state, the covariance $\Pi_\xi = E[\xi_t \xi_t']$ satisfies a Lyapunov equation $\Pi_\xi = A\Pi_\xi A' + Q_w$.

Proof. We have

$$\begin{aligned}
 \xi_{t+1} - A\xi_t &= Ax_t + Bu_t + K\epsilon_t - Mu_{t+1} - Ax_t + AMu_t \\
 &= Bu_t + K\epsilon_t - M(A_u u_t + v_t) + AMu_t \\
 &= (B - MA_u + AM)u_t + K\epsilon_t - Mv_t \\
 &= K\epsilon_t - Mv_t = w_t,
 \end{aligned}$$

as quoted. □

The new algorithm is enabled by the following result.

Result II. $(A, Q_w^{\frac{1}{2}})$ is reachable.

Proof. Suppose $(A, Q_w^{\frac{1}{2}})$ is not reachable. Then there exists left eigenvector v of A with eigenvalue λ , i.e. $v'A = \lambda v'$ so that $v'Q_w^{\frac{1}{2}} = 0$. But then $v'Q_w v = v'KQ_\epsilon K'v + v'MQ_v M'v = 0$. But Q_ϵ, Q_v are positive definite so we must have $v'K = 0, v'M = 0$. Left multiplying by v' in the Sylvester equation (5.2) yields $v'AM - v'MA_u + v'B = 0 \Rightarrow v'B = -\lambda v'M = 0$. So $v'B = 0, v'K = 0$ which contradicts the reachability of $(A, [K, B])$ in A1. The result follows. □

Remark 3. In view of Remark 2(iv), by properties of the Lyapunov equation [11, Lemma D.1.2(v)] and Result II we conclude that Π_ξ is positive definite.

5.2 The Closed-Form Stable Estimators

We now develop the closed-form stable estimators for both A_u and A . We first extract an estimator $\check{\xi}_t$ of the latent Markovian state and then apply the correlation stable estimators as follows.

S⁵ Algorithm.

Closed-form Stable State Space SubSpace Algorithm.

The closed-form algorithm is in two parts.

(I) \hat{A}_u : The closed-form stable estimator for A_u :

Let $\bar{U} = [u_0, \dots, u_{\bar{T}}]$ and \bar{U}_1 be \bar{U} without the first column and \bar{U}_0 be \bar{U} without the last column. Define $S_{u,ij} = \frac{1}{\bar{T}} \bar{U}_i \bar{U}'_j, i, j \in \{0, 1\}$. Then

$$\hat{A}_u = S_{u,10} S_{u,00}^{-\frac{1}{2}} S_{u,11}^{-\frac{1}{2}}, \quad (5.4)$$

is a CS estimator of A_u .

(II) \hat{A} : The closed-form stable estimator for A :

Let $\hat{X} = [\hat{x}_p, \dots, \hat{x}_{p+T}] \in \mathbb{R}^{\hat{n} \times (T+1)}$ be the state estimators from S⁴ and \hat{A}_*, \hat{B} be the LS estimators given in (3.8), where \hat{A}_* may be unstable. Then solve for \hat{M} the Sylvester equation

$$\hat{A}_* \hat{M} - \hat{M} \hat{A}_u + \hat{B} = 0. \quad (5.5)$$

Now construct the estimated transformed state sequence

$$\check{\xi}_t = \hat{x}_t - \hat{M} u_t, \quad (5.6)$$

for $t = p, \dots, p + T$. Define $\check{Z}, \check{Z}_1, \check{Z}_0$ and $\check{S}_{\xi,ij}$ analogously to Z, Z_1, Z_0 and $S_{\xi,ij}$ in (4.2), respectively, but replacing ξ_t by $\check{\xi}_t$. Then the CS estimator of A is given by

$$\hat{A} = \check{S}_{\xi,10} \check{S}_{\xi,00}^{-\frac{1}{2}} \check{S}_{\xi,11}^{-\frac{1}{2}}, \quad (5.7)$$

Remarks 4.

- (i) The stability of \hat{A}_u follows directly from Theorem 1 since u_t is observed. The stability of \hat{A} also follows since replacing the true states with the estimated ones does not affect the proof of stability in Theorem 1.
- (ii) The computational cost of solving the Sylvester equation is minor.
- (iii) The Sylvester equation (5.5) has a unique solution iff \hat{A}_* and \hat{A}_u have no common eigenvalues. This holds w.p.1 because, as proved below, they are consistent estimators so they can not accumulate mass other than at the true eigenvalues which are distinct by A3.

6 Asymptotic Analysis

In this section, we develop the strong consistency for \hat{A}_u and \hat{A} . Since $\hat{B}, \hat{C}, \hat{K}$ are least squares estimators, their consistency will follow from the works we cite below, i.e. [1], [22]. We now obtain, for the first time, strong consistency results for a guaranteed stable system matrix estimator of an IO-SS system.

Throughout this section, we assume

- (a) the true model order n is known, i.e. $\hat{n} = n$.
- (b) the past lag $p \rightarrow \infty$ at a certain rate (see below).

We introduce the big-O notation. A function $g_T = O(\gamma_T)$ if there exists a constant c such that $\limsup_T |g_T|/\gamma_T \leq c < \infty$ holds w.p.1. We also introduce $\gamma_T = \sqrt{\log \log T/T}$.

6.1 Preliminary Consistency Results

Our theorems rely on two fundamental sets of results for LS estimators as follows.

Theorem 2. [8] Consider the VAR(1) input signal obeying A3. Introduce the LS estimator of A_u , namely, $\hat{A}_{u*} = S_{u,10} S_{u,00}^{-1}$. Then the following results hold w.p.1.

- (a) Any eigenvalue λ_0 of $S_{u,00}$ satisfies $0 < a_0 < \lambda_0 < b_0 < \infty$, for some constants a_0, b_0 .
- (b) Any eigenvalue λ_1 of $S_{u,11}$ satisfies $0 < a_1 < \lambda_1 < b_1 < \infty$, for some constants a_1, b_1 .
- (c) $\|S_{u,00}\| = O(1), \|S_{u,11}\| = O(1), \|S_{u,10}\| = O(1)$.
- (d) $\|\hat{A}_{u*}\| = O(1)$.

Further, the following strong consistency results hold w.p.1. as $\bar{T} \rightarrow \infty$.

- (e) $\|S_{u,00} - \Pi_u\| = O(\gamma_{\bar{T}}), \|S_{u,11} - \Pi_u\| = O(\gamma_{\bar{T}}),$
 $\|S_{u,10} - \Pi_{u,10}\| = O(\gamma_{\bar{T}}).$
- (f) $\|\hat{A}_{u*} - A_u\| \leq O(\gamma_{\bar{T}}).$

Corollary 2. Results (a),(b),(c),(e) also hold for ξ_t of Theorem 2, i.e. $S_{\xi,00}, S_{\xi,11}, S_{\xi,10}$ obey the corresponding results.

Proof. This follows from Remarks 1(ii) following assumption A3 from which it follows that ξ_t obeys A2.

Theorem 3. [22] Suppose the input process u_t is generated by (2.2) satisfying assumption A3 and the output process y_t is generated by (2.1) satisfying assumption A1. Also assume that the true model order is known such that $\hat{n} = n$ and in the S^4 steps, the future lag $f \geq n$ is fixed and finite, and the past lag $p = p_T$ is chosen such that for some finite α , $p_T/(\log T)^\alpha \rightarrow 0$ w.p.1, as $p_T \rightarrow \infty$. Introduce $\Gamma = \hat{\mathcal{O}}_f^\dagger \mathcal{O}_f$. The following results hold w.p.1.

$$(a) \quad \|\hat{A}_*\| = O(1), \|\hat{B}\| = O(1), \\ \|\Gamma\| = O(1), \|\Gamma^{-1}\| = O(1).$$

Further, the following strong consistency results hold w.p.1. as $T \rightarrow \infty$.

$$(b) \quad T^{-\frac{1}{2}}\|\hat{X} - \Gamma X\| \leq p_T O(\gamma_T).$$

$$(c) \quad \|\hat{A}_* - \Gamma A \Gamma^{-1}\| \leq p_T O(\gamma_T).$$

$$(d) \quad \|\hat{B} - \Gamma B\| \leq p_T O(\gamma_T).$$

Remark 5. In [22], the results are developed when $f_T = p_T \rightarrow \infty$ under the rate specified above. Results for finite f can be proved without difficulty.

6.2 \hat{A}_u Consistency

We now develop consistency for the closed-form stable estimator \hat{A}_u .

Result III. Strong Consistency of \hat{A}_u . Under A3, $\|\hat{A}_u - A_u\| \leq O(\gamma_{\bar{T}})$ w.p.1 as $\bar{T} \rightarrow \infty$.

Proof. We have $\|\hat{A}_u - A_u\| \leq \|\hat{A}_u - \hat{A}_{u*}\| + \|\hat{A}_{u*} - A_u\|$. But by Theorem 2(f), $\|\hat{A}_{u*} - A_u\| \leq O(\gamma_{\bar{T}})$. We now show that $\|\hat{A}_u - \hat{A}_{u*}\| \leq O(\gamma_{\bar{T}})$ yielding the result. We have

$$\begin{aligned} \|\hat{A}_u - \hat{A}_{u*}\| &= \|\hat{A}_{u*} S_{u,00}^{\frac{1}{2}} S_{u,11}^{-\frac{1}{2}} - \hat{A}_{u*}\| \\ &= \|\hat{A}_{u*} (S_{u,00}^{\frac{1}{2}} - S_{u,11}^{\frac{1}{2}}) S_{u,11}^{-\frac{1}{2}}\| \\ &\leq \|\hat{A}_{u*}\| \|S_{u,00}^{\frac{1}{2}} - S_{u,11}^{\frac{1}{2}}\| \|S_{u,11}^{-\frac{1}{2}}\| \end{aligned}$$

Applying a perturbation bound on matrix square roots [27, Lemma 2.2] we find

$$\begin{aligned} \|S_{u,00}^{\frac{1}{2}} - S_{u,11}^{\frac{1}{2}}\| &\leq \frac{1}{a_0 + a_1} \|S_{u,00} - S_{u,11}\| \\ &\leq \frac{1}{a_0 + a_1} (\|S_{u,00} - \Pi_u\| + \|S_{u,11} - \Pi_u\|) \\ &= O(\gamma_{\bar{T}}), \end{aligned}$$

where $a_0 > 0$ and $a_1 > 0$ uniformly bound the eigenvalues of $S_{u,00}$ and $S_{u,11}$ from below, respectively, in view of Theorem 2(a,b). Note that by Theorem 2(c,d), $\|\hat{A}_{u*}\| = O(1)$, $\|S_{u,11}\| = O(1) \Rightarrow \|S_{u,11}^{-\frac{1}{2}}\| = O(1)$. It follows that $\|\hat{A}_u - \hat{A}_{u*}\| \leq O(\gamma_{\bar{T}})$. \square

6.3 \hat{A} Consistency

To proceed we need some further preliminary results.

Result IV. Under A1-A3, the following strong consistency results hold w.p.1. as $T \rightarrow \infty$.

- (a) $\|\hat{M} - \Gamma M\| \leq p_T O(\gamma_T)$.
- (b) $T^{-\frac{1}{2}} \|\check{Z} - \Gamma Z\| \leq p_T O(\gamma_T)$.
- (c) $\|\check{S}_{\xi,00} - \Gamma \Pi_{\xi} \Gamma'\| \leq p_T O(\gamma_T)$
 $\|\check{S}_{\xi,11} - \Gamma \Pi_{\xi} \Gamma'\| \leq p_T O(\gamma_T)$,
 $\|\check{S}_{\xi,10} - \Gamma \Pi_{\xi,10} \Gamma'\| \leq p_T O(\gamma_T)$.

Proof.

(a) Let $\hat{G} = I_m \otimes \hat{A}_* - \hat{A}_u \otimes I_n$ and $G = I_m \otimes \Gamma A \Gamma^{-1} - A_u \otimes I_n$. Using the vec operator solution to the Sylvester equation, we find

$$\begin{aligned} \|\hat{M} - \Gamma M\| &= \|\text{vec}(\hat{M} - \Gamma M)\| \\ &= \|\hat{G}^{-1} \text{vec}(\hat{B}) - G^{-1} \text{vec}(\Gamma B)\| \\ &\leq \|\hat{G}^{-1} - G^{-1}\| \|\hat{B}\| + \|G^{-1}\| \|\hat{B} - \Gamma B\|. \end{aligned}$$

However, $\|\hat{B}\| = O(1)$, $\|G^{-1}\| = O(1)$, $\|\hat{B} - \Gamma B\| \leq p_T O(\gamma_T)$ by Theorem 3(a,d) and Theorem 2(d). Next

$$\begin{aligned} \|\hat{G}^{-1} - G^{-1}\| &= \|\hat{G}^{-1}(\hat{G} - G)G^{-1}\| \\ &\leq \|\hat{G}^{-1}\| \|\hat{G} - G\| \|G^{-1}\|, \end{aligned}$$

where $\|G^{-1}\| = O(1)$, $\|\hat{G}^{-1}\| = O(1)$. Now we write

$$\begin{aligned}\|\hat{G} - G\| &= \|I_m \otimes (\hat{A}_* - \Gamma A \Gamma^{-1}) - (\hat{A}_u - A_u) \otimes I_n\| \\ &\leq \|I_m \otimes (\hat{A}_* - \Gamma A \Gamma^{-1})\| + \|(\hat{A}_u - A_u) \otimes I_n\| \\ &= \sqrt{m} \|\hat{A}_* - \Gamma A \Gamma^{-1}\| + \sqrt{n} \|\hat{A}_u - A_u\| \\ &\leq p_T O(\gamma_T).\end{aligned}$$

Combining these bounds yields result (a).

(b) We have $\check{\xi}_t = \hat{x}_t - \hat{M}u_t$ and $\xi_t = x_t - Mu_t$. Thus, $\check{Z} = \hat{X} - \hat{M}U$ and $Z = X - MU$, where $U = [u_p, \dots, u_{p+T}]$. So

$$\begin{aligned}rcl \check{Z} - \Gamma Z &= \hat{X} - \Gamma X - (\hat{M} - \Gamma M)U \\ \Rightarrow \frac{1}{\sqrt{T}} \|\check{Z} - \Gamma Z\| &\leq \frac{1}{\sqrt{T}} \|\hat{X} - \Gamma X\| + \|\hat{M} - \Gamma M\| \frac{\|U\|}{\sqrt{T}} \\ &\leq p_T O(\gamma_T) + p_T O(\gamma_T) \frac{\|U\|}{\sqrt{T}}\end{aligned}$$

by Theorem 3(b) and result (a). Continuing, via Theorem 2

$$\begin{aligned}rcl \frac{\|U\|^2}{T} &\leq \frac{1}{T} \|S_{u,11} - \Pi_u\| + \|\Pi_u\| + \frac{1}{T} \|u_0\|^2 \\ &\leq p_T O(\gamma_T) + O(1) + O(1/T) = O(1),\end{aligned}$$

and the quoted bound follows.

(c) Consider $\check{S}_{\xi,00}$ for example. First write

$$\begin{aligned}&\|\check{S}_{\xi,00} - \Gamma \Pi_\xi \Gamma'\| \\ &= \|(\check{S}_{\xi,00} - \Gamma S_{\xi,00} \Gamma') + (\Gamma S_{\xi,00} \Gamma' - \Gamma \Pi_\xi \Gamma')\| \\ &\leq \|\check{S}_{\xi,00} - \Gamma S_{\xi,00} \Gamma'\| + \|\Gamma\|^2 \|S_{\xi,00} - \Pi_\xi\|.\end{aligned}\tag{6.1}$$

We need to show both norms decay to 0. For the first norm, write

$$\begin{aligned}\check{S}_{\xi,00} - \Gamma S_{\xi,00} \Gamma' &= \frac{1}{T} (\hat{Z}_0 \hat{Z}_0' - \Gamma Z_0 Z_0' \Gamma') \\ &= \frac{1}{T} (\hat{Z}_0 - \Gamma Z_0) (\hat{Z}_0 - \Gamma Z_0)' \\ &\quad + \frac{1}{T} (\Gamma Z_0 \hat{Z}_0' + \hat{Z}_0 Z_0' \Gamma' - 2\Gamma Z_0 Z_0' \Gamma').\end{aligned}$$

We have $\|\frac{1}{T} (\hat{Z}_0 - \Gamma Z_0) (\hat{Z}_0 - \Gamma Z_0)'\| \leq p_T^2 O(\gamma_T^2)$ by result (b). For the remaining

terms, we have

$$\begin{aligned} \left\| \frac{1}{T} (\hat{Z}_0 Z_0' - \Gamma Z_0 Z_0') \Gamma' \right\| &= \| T^{-\frac{1}{2}} (\hat{Z}_0 - \Gamma Z_0) T^{-\frac{1}{2}} Z_0' \Gamma' \| \\ &\leq \| T^{-\frac{1}{2}} (\hat{Z}_0 - \Gamma Z_0) \| \| T^{-\frac{1}{2}} Z_0 \| \| \Gamma \|. \end{aligned}$$

We have $\| T^{-\frac{1}{2}} (\hat{Z}_0 - \Gamma Z_0) \| \leq p_T O(\gamma_T)$ by result (b) and $\| \Gamma \| = O(1)$ by Theorem 3(a). But $\| T^{-\frac{1}{2}} Z_0 \| = \| T^{-\frac{1}{2}} (\hat{X}_0 - \hat{M} U_0) \| \leq \| T^{-\frac{1}{2}} \hat{X}_0 \| + \| \hat{M} \| \| T^{-\frac{1}{2}} U_0 \|$. We have $\| \hat{M} \| = O(1)$, because norms of \hat{A}_* , \hat{A}_u , \hat{B} are all bounded, and also $\| T^{-\frac{1}{2}} U_0 \| = O(1)$ by Theorem 2(c). Now note that $\hat{X} = \hat{\mathcal{K}}_p Z_p^-$. In [22], it is shown that $\| \hat{\mathcal{K}}_p \| = O(1)$ (above their eq.39), and $T^{-1} Z_p^- (Z_p^-)' = O(1)$ (their eq.28). Thus, $\| T^{-\frac{1}{2}} \hat{X}_0 \| = O(1)$ so the above norm decays at a rate of $p_T O(\gamma_T)$. It then follows that $\| \check{S}_{\xi,00} - \Gamma S_{\xi,00} \Gamma' \| \leq p_T O(\gamma_T)$.

Now for the second norm in (6.1), note that ξ_t is a VARMA process generated by the joint innovation $[e_t', v_t']'$ which satisfies A2. Then $\| \frac{1}{T} \sum_{t=p}^{p+T-1} \xi_{t+i} \xi_t' - E[\xi_{t+i} \xi_t'] \| \leq O(\gamma_T)$ w.p.1, for $|i| \leq (\log T)^\alpha$, for any α (see [8] or [22, eq.26]). Then taking $i = 0$, we have $\| S_{\xi,00} - \Pi_\xi \| \leq O(\gamma_T)$. Combining the above yields the result for $\check{S}_{\xi,00}$. Results for $\check{S}_{\xi,10}$ and $\check{S}_{\xi,11}$ follow analogously. \square

We can now study the consistency of \hat{A} .

Result V. Consistency of \hat{A} .

Assume A1,A2,A3 hold. Also assume:

- (i) the true model order is known so that $\hat{n} = n$;
- (ii) the future lag $f \geq n$ is fixed and finite;
- (iii) the past lag $p = p_T$ is chosen such that $p_T / (\log T)^\alpha \rightarrow 0$ w.p.1, as $p_T \rightarrow \infty$, for some finite α .

Then, $\hat{A} \rightarrow A$ w.p.1. Further, $\| \hat{A} - \Gamma A \Gamma^{-1} \| \leq p_T O(\gamma_T)$, w.p.1, as $T \rightarrow \infty$.

Proof. Decompose $\hat{A} - \Gamma A \Gamma^{-1} = \alpha + \beta - \delta$, where

$$\begin{aligned} \alpha &= (\check{S}_{\xi,10} - \Gamma \Pi_{\xi,10} \Gamma') (\Gamma \Pi_\xi \Gamma')^{-1} \\ \beta &= \check{S}_{\xi,10} [\check{S}_{\xi,00}^{-1} - (\Gamma \Pi_\xi \Gamma')^{-1}] \\ \delta &= \check{S}_{\xi,00}^{-\frac{1}{2}} (\check{S}_{\xi,00}^{-\frac{1}{2}} - \check{S}_{\xi,11}^{-\frac{1}{2}}). \end{aligned}$$

Then use the norm inequalities and Result IV(c) and take analogous steps to treat the matrix inverse and square root as in previous proofs to get the quoted result. \square

Remarks 6.

- (a) The condition that the future lag f also tends to infinity is a stronger assumption, under which the same results hold.
- (b) The stable, closed-form estimator in [14] is shown to be consistent when both $f \rightarrow \infty, p \rightarrow \infty$ but it has an asymptotic bias when f is finite [1, Theorem 3].

7 Simulations

We compare both the precision and computational effort of our S^5 against the existing algorithms that guarantee system stability, with a SS model order n up to 1024. We omit discussions about \hat{A}_u and concentrate here on the IO-SS estimates since \hat{A}_u is a pure VAR(1) stable estimator and has already been discussed in simulations in [24].

In [23], we compared our FB estimator for N-SS models against various algorithms and found the SDP [16] to be the most competitive. Thus, we include here the SDP method, but we use a version for IO-SS [12]. More recent developments include the LQR method [10] and the category of ‘nearest-stable’ algorithms: Orth [19], FGM [7], SuccConv [21]. However, the LQR method only treats a VAR(1) process without an input and needs the noise covariance to be pd. Thus, we are unable to apply this method to our problem. The ‘nearest-stable’ algorithms are developed without system context and are not for SS models. We also found some fundamental problems for such methods (see below). However, because they are the more recent stability-guaranteed algorithms and also because it is not hard to amend them to fit a SS model, we feel compelled to include them in the simulations.

Thus, we will compare our (a) S^5 to (b) Orth, (c) FGM, (d) SDP.

We emphasize here that expect our S^5 which is closed-form, all algorithms have multiple tuning parameters.

- Orth uses Riemannian trust-regions solver whose tuning parameters include initial iterate, convergence tolerance, trust-region radiuses, accept/reject threshold, etc.
- FGM has tuning parameters: initial iterate (very sensitive), eigenvalue bounds, fast gradient method step size, line-search parameters, etc.
- SDP has tuning parameters: left and right weighting matrices, scaling parameter in the Lyapunov equation, etc.

Besides, more needs to be addressed about the ‘nearest-stable’ algorithms.

7.1 Pre-Simulation Discussions on the ‘Nearest-Stable’ Algorithms

The ‘nearest-stable’ algorithms seek to minimize $\|A_s - \hat{A}_*\|$, the Frobenius distance between a given unstable matrix \hat{A}_* to the stable A_s in the (non-convex and non-smooth) set of stable real matrices. Some problems have already been pointed out by their authors, e.g. they are only able to find a local minimum [19] [7] [21] and some algorithms scale badly to higher matrix dimensions [19]. However, what lacks discussion is their ignorance of the system context. We address three main points.

(1) *Incorrect weighting:* Consider the one-step mean square error $\|Z_1 - A_s Z_0\| = \|Z_1 - \hat{A}_* Z_0 + (\hat{A}_* - A_s) Z_0\| \leq \|Z_1 - \hat{A}_* Z_0\| + \|(\hat{A}_* - A_s) Z_0\|$. Then the perturbation should be weighted as $\|(\hat{A}_* - A_s) S_{00}^{\frac{1}{2}}\|$.

(2) *Distorted poles:* As discussed in [19], the ‘nearest-stable’ algorithms tend to put the dominating pole very close to the unit circle, e.g. at $1 - 10^{-10}$, distorting pole locations and risking instability due to rounding errors. Solving a Lyapunov equation $P = A_s P A_s' + Q$ also needs extra attention in this case.

(3) *Orthogonal similarities:* Different ‘nearest-stable’ algorithms yield solutions with nearly identical perturbation norms but vastly different orientations. This inconsistency can affect the basis of the estimated A in SS identification.

For example, the unstable matrix $\begin{bmatrix} 2 & 2 & 2 \\ 2 & 2 & 2 \\ 2 & 2 & 2 \end{bmatrix}$, considered in [19] and [7], has

solutions:

- [19] a seemingly global minimizer $\begin{bmatrix} 1 & 2 & 2 \\ 0 & 1 & 2 \\ 0 & 0 & 1 \end{bmatrix}$

with objective norm 15 ,

- [19] the Orth solution $\begin{bmatrix} 1.0000 & 0.9550 & 1.5848 \\ 1.0450 & 1.0000 & 2.6297 \\ 0.4152 & -0.6297 & 1.0000 \end{bmatrix}$

with objective norm $15 + 10^{-15}$, and

- [7] the FGM solution $\begin{bmatrix} 0.9969 & 1.4010 & 0.7688 \\ 0.5544 & 0.9878 & -0.6507 \\ 1.2476 & 2.6740 & 1.0112 \end{bmatrix}$

with objective norm 15.02 .

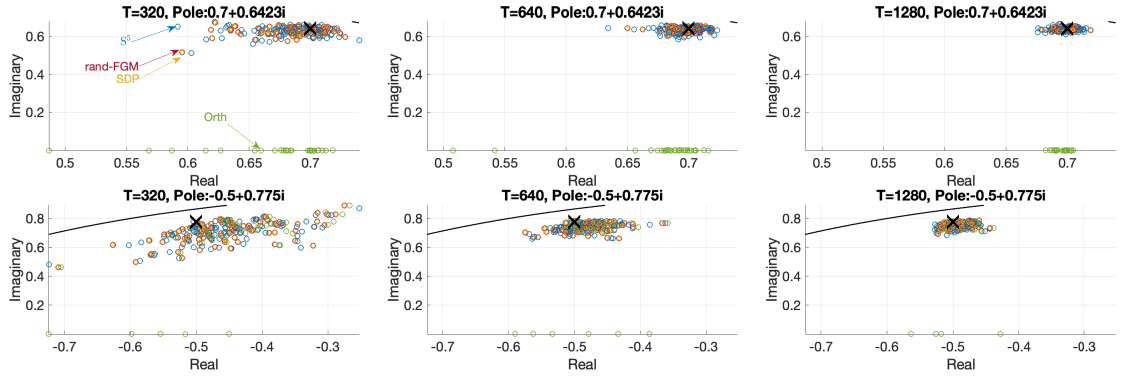


Figure 1: Locations of the estimated complex poles for $n = 5$: Poles for S^5 , rand-FGM and SDP cluster closely around the true ones. Poles for rand-FGM and SDP almost overlap. However, a large number of poles for Orth lie on the real axis yielding a large discrepancy.

Despite minimal differences in perturbation norms, these matrices are oriented differently, causing inconsistencies in SS identification estimates.

These weaknesses of the ‘nearest-stable’ algorithms will be exposed in the following simulations.

7.2 Low Dimensional Simulations

We first consider a low dimensional 2-input-1-output ($m = 2, d = 1$) SS system with order $n = 5$ and set the following true system matrices.

$$A = \begin{bmatrix} 0.7 & 0.642 & 0 & 0 & 0 \\ -0.642 & 0.7 & 0 & 0 & 0 \\ 0 & 0 & -0.5 & 0.775 & 0 \\ 0 & 0 & -0.775 & -0.5 & 0 \\ 0 & 0 & 0 & 0 & -0.995 \end{bmatrix}$$

$$B = [0.2 \ 0.2 \ 0.2 \ 0.2 \ 0.2]', \quad C = [0.3 \ 0.3 \ 0.3 \ 0.3 \ 0.3]$$

$$K = [0.5 \ 0.5 \ -0.3 \ -0.3 \ -0.9]', \quad Q_\epsilon = 1$$

$$A_u = \begin{bmatrix} 0.9 & 0.2 \\ -0.2 & 0.9 \end{bmatrix}, \quad Q_v = \begin{bmatrix} 1 & 0.5 \\ 0.5 & 2 \end{bmatrix}.$$

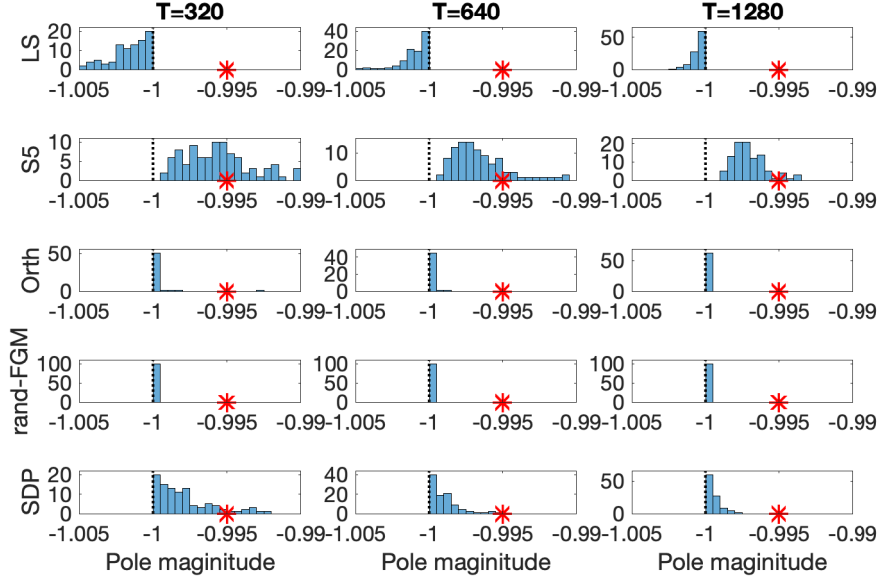


Figure 2: Histograms of the estimated real dominating poles for $n = 5$: We select LS estimates that are unstable. The ‘*’ marks are the true dominating pole. All four algorithms guarantee system stability. Orth and rand-FGM tend to put the eigenvalues on the unit circle, yielding inaccurate system dynamics. SDP also has such a trend as \bar{T} grows. However, S^5 does not.

System poles are -0.995 , $0.95e^{\pm j0.74}$, $0.92e^{\pm j}$. $\bar{A} = A - KC$ has eigenvalues 0.686 , $0.803e^{\pm j0.917}$, $0.821e^{\pm j1.11}$.

We use the CVA subspace algorithm to get the state estimates \hat{X} . We set the future lag $f = 10$ and vary $\bar{T} = 320, 640, 1280$. We set the past lag $p = \lceil 5 \ln \bar{T} \rceil = 29, 33, 36$ for each \bar{T} .

Since all algorithms use unstable LS estimates as initial values, we simulate a large number of repeats until there are 100 unstable LS estimates for each \bar{T} . The empirical probabilities of having one unstable LS estimate are 5.24%, 1.43%, 0.069% for $\bar{T} = 320, 640, 1280$, respectively.

We identify the stable estimates for A using the above 4 algorithms. We implement Orth and FGM on SS identification by simply replacing the unstable LS estimates of A by their ‘nearest’ stable estimates. FGM is found to be most reliable when it tries random initial guesses of the stable matrix and picks the best one [19] [7]. So we do the same and call it rand-FGM. MATLAB code for Orth and rand-FGM is available online [18] [6]. Other tuning parameters,

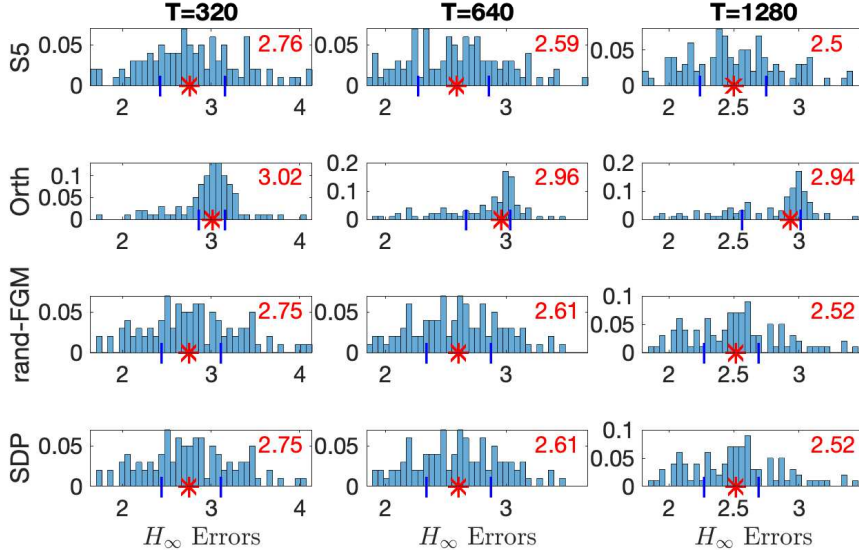


Figure 3: Histograms of the soft H_∞ error $e_3 = \sup_{\omega \in [0,3]} \bar{\sigma}(\hat{F}(\omega) - F(\omega))$ for $n = 5$: The medians are indicated by “*” marks and the number at the upper right corner of each histogram. The upper and lower quartiles are indicated by “|” marks.

e.g. step sizes and convergence tolerances, of the Orth and rand-FGM are set as default. For SDP, we take the identity matrix as the weighting matrices and set the scale parameter to be 10^{-8} .

7.2.1 Inspection of Poles

We first plot the pole locations of the estimated A matrices in Fig. 1 for complex poles and the pole histograms for the real dominating pole in Fig. 2.

From Fig. 1, we observe that expect for Orth, the estimated non-dominating poles cluster closely around the true ones. However, Orth prefers real poles which diverge far apart from the true poles. This is the same observation in their original paper [19, Fig. 8].

An inspection of Fig. 2 yields that all algorithms move the unstable LS poles inside the unit circle. However, Orth and rand-FGM tend to put poles very close to the unit circle. The percentages of poles with magnitudes greater than $1 - 10^{-10}$ for $\bar{T} = 320, 640, 1280$ are:

- Orth: 87%, 88%, 85%, respectively.

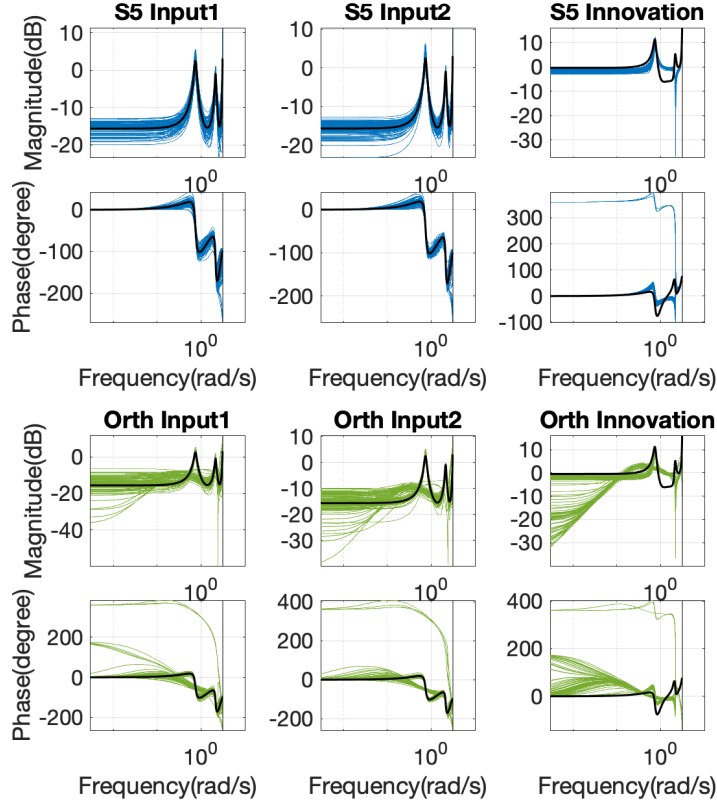


Figure 4: 100 estimated bode plots in frequency range $\omega \in [0, 3]$ for $\bar{T} = 1280$ for $n = 5$: True bode plots are black. The bode plots for rand-FGM and SDP resemble closely to those of S^5 and are thus omitted. In the undisplayed range $\omega \in (3, \pi]$, the peak magnitudes are around 45dB, 300dB, 200dB and 110dB for S^5 , Orth, rand-FGM and SDP, respectively.

- rand-FGM: 52%, 62%, 98%, respectively.

The above percentages are 0% for S^5 and SDP. However, SDP also has the same trend as \bar{T} increases. A close inspection of S^5 histograms shows that the largest magnitude of the estimated dominating pole is, on the contrary, decreasing as \bar{T} increases, approaching closer to the true dominating pole. We need to emphasize that from the histograms, it may seem the S^5 estimators are not statistically consistent, but that is because the plots are only for the small population (5.25% for $\bar{T} = 320$ and 0.069% for $\bar{T} = 1280$) of estimates where LS estimates are unstable.

7.2.2 H_∞ Errors

We want to quantify the estimation error. Denoting by \hat{A}_s any stable estimate from any algorithm, obvious choices are the perturbation mean squared error $\|\hat{A}_s - \hat{A}_*\|$ and the one-step-ahead prediction mean squared error $\|\hat{X}_1 - \hat{A}_s \hat{X}_0 - \hat{B}U_0\|$. However, the perturbation mean squared error has the described problems and the one-step-ahead prediction mean squared error does not fully depict the system dynamics; multi-step-ahead prediction error should also be considered. Thus, we consider the frequency behaviors and define the (hard) H_∞ error

$$e = \sup_{\omega \in [0, \pi]} \bar{\sigma}(\hat{F}(\omega) - F(\omega)),$$

where we have assumed the sampling frequency to be 1 and $\bar{\sigma}(\cdot)$ denotes the largest singular value, $F(\omega) = C(e^{j\omega}I - A)^{-1}[B, K] + [0_{d \times m}, I_d]$ is the true frequency response of the whole SS system (A, B, C, K) , and $\hat{F}(\omega) = \hat{C}(e^{j\omega}I - \hat{A}_s)^{-1}[\hat{B}, \hat{K}] + [0_{d \times m}, I_d]$ is the estimated frequency response. However, inspecting the estimated poles suggests that when $\omega \approx \pi$, the hard H_∞ error e will be extremely large for Orth and rand-FGM since the estimated dominating poles are nearly on the unit circle, undermining good approximation at other frequencies. We thus also introduce the soft H_∞ error

$$e_{\omega_*} = \sup_{\omega \in [0, \omega_*]} \bar{\sigma}(\hat{F}(\omega) - F(\omega)).$$

We find taking $\omega_* = 3$ best separates the well-approximated frequencies from those with an exploding response.

We calculate both hard and soft H_∞ errors by sampling the frequency responses on 1000 points over the corresponding frequency range. We plot the histograms of the soft H_∞ errors e_3 in Fig. 3 and the estimated bode plots on top of the true ones in Fig. 4. We only plot the bode plots for $\bar{T} = 1280$ due to space limits. We also omit the bode plots for rand-FGM and SDP, since they resemble closely to those of S⁵ in the well-approximated frequency range. The hard H_∞ errors differ greatly among the algorithms so they are summarized in Table. 1 as a better way of display.

From Fig. 3 and Fig. 4, it is observed that S⁵, rand-FGM and SDP have nearly equally good performance in the well-approximated frequency region measured by the soft H_∞ error whereas Orth shows a great discrepancy in

Medians	S ⁵	Orth	rand-FGM	SDP
$T = 320$	37.8	7.2×10^{14}	2.7×10^9	90.6
$T = 640$	34.6	5.9×10^{14}	3.6×10^9	229
$T = 1280$	28.6	5.9×10^{14}	2.9×10^9	583

Table 1: Medians of the hard H_∞ errors $e = \sup_{\omega \in [0, \pi]} \bar{\sigma}(\hat{F}(\omega) - F(\omega))$ for $n = 5$.

Total comp. time (s)	S ⁵	Orth	rand-FGM	SDP
$T = 320$	0.0170	5.40	11.4	1.26
$T = 640$	0.0232	5.27	11.9	1.30
$T = 1280$	0.0340	5.08	15.9	1.14

Table 2: Total computational times (s) for 100 repeats for $n = 5$.

the spectra resulting in the largest soft H_∞ errors, because it tends to put the non-dominating poles on the real axis. For the response around the frequency π , inspection of Table. 1 yields clearly that S⁵ performs the best yielding magnitudes smaller hard H_∞ errors than the other methods. Also, the increasing hard H_∞ errors of SDP as \bar{T} grows confirms the trend of its estimated dominating pole moving closer to the unit circle whereas our S⁵ has decreasing errors. Interestingly, our S⁵ estimates are by no means the ‘nearest’ to the LS estimate but nonetheless have the best performance.

7.2.3 Computational times

Computational times are summarized in Table. 2. Our S⁵ computes magnitudes faster than the iterative algorithms.

7.3 High Dimensional Simulations

Aside from the superiority of S⁵ in both accuracy and computational efficiency, S⁵ scales easily to huge dimension identification. We illustrate this by considering model orders $n = 16, 64, 256, 1024$.

However, we only compare our S⁵ with rand-FGM here because in our previous work [23], we showed that SDP can not handle system orders $n \geq 250$, and in [19], it was noted that Orth can only handle system orders up to $n \approx 100$.

We design the true SS parameters as follows. We fix $d = 1$ and $m = 2$ and use the same A_u and Q_v as in the low-dimensional simulations. We put

all system poles at the magnitude of 0.9999 around the circle and set A to be a block diagonal matrix. Each 2×2 block contains the real part of a pair of complex conjugate eigenvalues on its diagonal and the imaginary parts at its off-diagonal entries. We set all entries in B to 0.2 and those in C to 0.3. We choose the past and future lags $f = p = n + 10$ and consider $\bar{T} = \lceil 5(m + 2)f + 500 \rceil$. We set K such that the the eigenvalues of $\bar{A}^p = (A - KC)^p$ have magnitude 0.1. Such magnitude is neither too small so that the fit is too good to generate a single unstable LS estimate nor too big so that S^4 generates bad estimates of the states (please refer to equation (3.1) and the discussions below). We simulate 50 unstable LS estimates for each n . The empirical probabilities of getting one unstable LS estimate are 57.1%, 94.3%, 87.7%, 3.1% for $n = 4, 16, 256, 1024$, respectively.

In the simulations, our S^5 computed very fast with all model orders (see below). However, rand-FGM converged in all simulations for $n = 16, 64$ but it only converged in 26 simulations for $n = 256$ and in 37 simulations for $n = 1024$. The unconverged simulations resulted in NaN (Not a Number).

We compare the converged estimates by

- in Fig. 5, the pole magnitude histograms,
- in Fig. 6, the (hard) H_∞ error boxplots, and
- in Table. 3, the average computational times.

We have the following observations.

Fig. 5 shows that the histograms of pole magnitudes of S^5 cluster closer around the true pole magnitude as the order n (as well as \bar{T} , noting \bar{T} is a function of n) increases. However, rand-FGM still puts the poles very close to the unit circle for $n = 16, 64, 256$.

From Fig. 6, S^5 has much better H_∞ errors for $n = 16, 64, 256$ compared with the converged estimates of rand-FGM. Rand-FGM outperforms S^5 in H_∞ errors when $n = 1024$ despite its poor convergence.

From Table 3, our S^5 takes nearly no time to calculate even when $n = 1024$, confirming the computational efficiency. However, rand-FGM takes hours for $n = 1024$ with poor convergence.

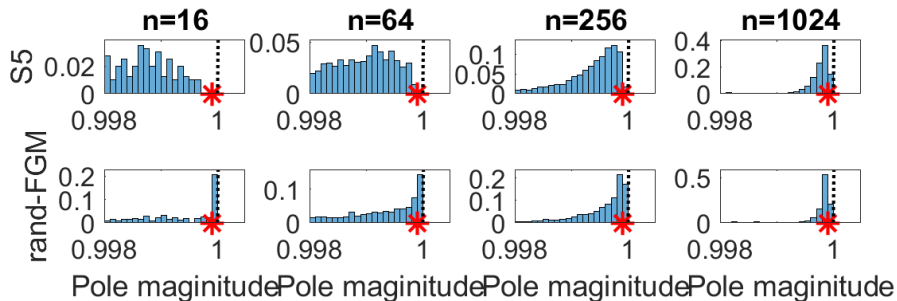


Figure 5: Histograms of the pole magnitudes in high dimensional simulations: The “*” marks are the true pole magnitude. The histograms for rand-FGM for $n = 256$ and $n = 1024$ use the 26 and the 37 converged estimates, respectively.

Ave. comp. time	S^5	rand-FGM
$n = 16$	8.6×10^{-4} s	0.17s
$n = 64$	4.7×10^{-3} s	8.4s
$n = 256$	0.12s	402s= 6.7mins
$n = 1024$	3.6s	8173s= 2.3hrs

Table 3: Average computational times in high-dimensional simulations: For $n = 256$ and $n = 1024$, the average for rand-FGM is taken with the 26 and the 37 converged estimates.

8 Conclusions

In this paper, we considered a stable state space subspace (S^5) identification of an input-output state-space model with a VAR(1) input. We developed closed-form, stability-guaranteed estimators for both the state space model and the VAR(1) coefficient, based on correlation stable estimators. We showed that our estimators are strongly consistent under minor conditions.

In comparative simulations, we considered both low- and high-dimensional cases with the model order up to $n = 1024$. We compared our estimator with the existing iterative algorithms and demonstrated the superiority of S^5 in both precision and computational cost.

For future work, a natural extension is to consider a VAR(p) input. However, the consistency proof will be much more complicated. We will pursue it elsewhere.

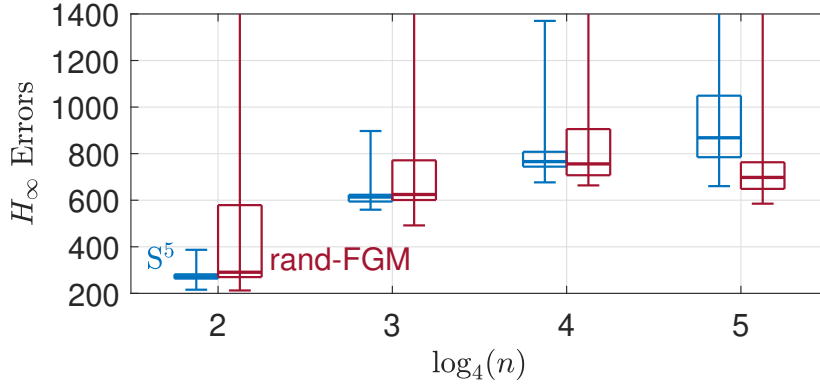


Figure 6: Boxplots of H_∞ errors in high-dimensional simulations: We only have 26 and 37 converged estimates with rand-FGM for $n = 256$ and $n = 1024$, respectively. The maximum H_∞ errors for rand-FGM for $n = 16, 64, 256, 1024$ are, respectively, 7400, 90407, 3738, 3481 and that for S^5 for $n = 1024$ is 2417; they are outside the range of the plot.

References

- [1] D. Bauer. Asymptotic properties of subspace estimators. *Automatica*, 41(3):359–376, 2005.
- [2] B. Boots, G. J. Gordon, and S. Siddiqi. A constraint generation approach to learning stable linear dynamical systems. *Advances in Neural Information Processing Systems*, 20, 2007.
- [3] J. P. Burg. *Maximum entropy spectral analysis*. Stanford University, 1975.
- [4] N. L. C. Chui and J. M. Maciejowski. Realization of stable models with subspace methods. *Automatica*, 32(11):1587–1595, 1996.
- [5] B. N. Datta. *Numerical Methods for Linear Control Systems*. Elsevier, 2004.
- [6] N. Gillis, M. Karow, and P. Sharma. Accompanying code for “approximating the nearest stable discrete-time system”. <https://sites.google.com/site/nicolasgillis/code>, 2019. [Online; accessed June-2024].
- [7] N. Gillis, M. Karow, and P. Sharma. Approximating the nearest stable discrete-time system. *Linear Algebra and its Applications*, 573:37–53, 2019.

- [8] E. J. Hannan and M. Deistler. *The Statistical Theory of Linear Systems*. SIAM, 2012.
- [9] Roger A. Horn and Charles R. Johnson. *Topics in Matrix Analysis*. Cambridge University Press, 1991.
- [10] W. Jongeneel, T. Sutter, and D. Kuhn. Efficient learning of a linear dynamical system with stability guarantees. *IEEE Trans. Autom. Contr.*, 68(5):2790–2804, 2023.
- [11] T. Kailath. *Linear estimation*. Prentice Hall, Upper Saddle River, New Jersey, 2000.
- [12] S. L. Lacy and D. S. Bernstein. Subspace identification with guaranteed stability using constrained optimization. *IEEE Trans. Autom. Contr.*, 48(7):1259–1263, 2003.
- [13] W. E. Larimore. System identification, reduced-order filtering and modeling via canonical variate analysis. In *American Control Conference*, pages 445–451. IEEE, 1983.
- [14] J. M. Maciejowski. Guaranteed stability with subspace methods. *Systems & Control Letters*, 26(2):153–156, 1995.
- [15] G. Mallet, G. Gasso, and S. Canu. New methods for the identification of a stable subspace model for dynamical systems. In *IEEE Workshop on Machine Learning for Signal Processing*, pages 432–437. IEEE, 2008.
- [16] J. Mari, P. Stoica, and T. McKelvey. Vector ARMA estimation: a reliable subspace approach. *IEEE Trans. Signal Process.*, 48(7):2092–2104, 2000.
- [17] N. Matni, A. Proutiere, A. Rantzer, and S. Tu. From self-tuning regulators to reinforcement learning and back again. In *IEEE CDC*, pages 3724–3740, 2019.
- [18] V. Noferini and F. Poloni. Accompanying code for “nearest ω -stable matrix via Riemannian optimization”. <https://github.com/fph/nearest-omega-stable>, 2020. [Online; accessed June-2024].
- [19] V. Noferini and F. Poloni. Nearest *omega*-stable matrix via Riemannian optimization. *Numerische Mathematik*, 148(4):817–851, 2021.

- [20] A. H. Nuttall. Multivariate linear predictive spectral analysis employing weighted forward and backward averaging: A generalization of Burg’s algorithm. Report, Naval Underwater System Center, London, 1976.
- [21] F.-X. Orbandexivry, Y. Nesterov, and P. Van Dooren. Nearest stable system using successive convex approximations. *Automatica*, 49(5):1195–1203, 2013.
- [22] K. Peterzell, W. Scherrer, and M. Deistler. Statistical analysis of novel subspace identification methods. *Signal Processing*, 52(2):161–177, 1996.
- [23] X. Rong and V. Solo. State space subspace noise modeling with guaranteed stability. In *Proc. IEEE CDC*, pages 4203–8208, 2023.
- [24] X. Rong and V. Solo. Stable, consistent, closed-form estimators for VAR(1). In *Proc. IEEE CDC*, page in press, 2024.
- [25] X. Rong and V. Solo. Stable reduced-rank VAR identification. *arXiv:2403.00237 [stat.ME]*, 2024.
- [26] X. Rong and V. Solo. Symmetric VAR(1) modelling with guaranteed stability. In *Proc. IEEE ICASSP*, pages 9786–9790, 2024.
- [27] B. A. Schmitt. Perturbation bounds for matrix square roots and Pythagorean sums. *Linear Algebra and its Applications*, 174:215–227, 1992.
- [28] O. Strand. Multichannel complex maximum entropy (autoregressive) spectral analysis. *IEEE Trans. Autom. Contr.*, 22(4):634–640, 1977.
- [29] H. Tanaka and T. Katayama. Stochastic subspace identification guaranteeing stability and minimum phase. *IFAC Proceedings Volumes*, 38(1):910–915, 2005.
- [30] J. Umenberger, J. Wågberg, I. R. Manchester, and T. B. Schön. Maximum likelihood identification of stable linear dynamical systems. *Automatica*, 96:280–292, 2018.
- [31] T. Van Gestel, J. A. K. Suykens, P. Van Dooren, and B. De Moor. Identification of stable models in subspace identification by using regularization. *IEEE Trans. Autom. Contr.*, 46(9):1416–1420, 2001.
- [32] P. Van Overschee and B. De Moor. *Subspace identification for linear systems: theory, implementation, applications*. Kluwer, Boston, 1996.